Open access • Journal Article • DOI:10.1103/PHYSREVB.67.153306

Magnetotransport properties of a polarization-doped three-dimensional electron slab in graded AlGaN — Source link

Debdeep Jena, Sten Heikman, James S. Speck, Arthur C. Gossard ...+3 more authors

Institutions: University of California, Santa Barbara

Published on: 29 Apr 2003 - Physical Review B (American Physical Society)

Title

Magnetotransport properties of a polarization-doped three-dimensional electron slab in graded AlGaN

Journal

Physical Review B, 67(15)

ISSN

1098-0121

Authors

Jena, D
Heikman, S
Speck, J S
et al.

Publication Date

2003-04-01

Peer reviewed

Magnetotransport properties of a polarization-doped three-dimensional electron slab in graded AlGaN

Debdeep Jena,* Sten Heikman, James S. Speck, Arthur Gossard, and Umesh K. Mishra
Department of Electrical and Computer Engineering and Materials Department, University of California, Santa Barbara, California 93106

Angela Link and Oliver Ambacher
Walter Schottky Institute, Am Coulombwall, 3 D-85748 Garching, Germany

(Received 15 October 2002; revised 3 March 2003; published 29 April 2003)

Shubnikov–de-Haas oscillation is observed in a polarization-doped three-dimensional electron slab in a graded $Al_xGa_{1-x}N$ semiconductor layer. The electron slab is generated by the technique of grading the polar semiconductor alloy with spatially changing polarization. Temperature-dependent oscillations allow us to extract an effective mass of $m^*=0.21m_0$. The quantum scattering time measured ($\tau_q=0.3$ ps) is close to the transport scattering time ($\tau_t=0.34$ ps), indicating the dominance of short-range scattering. Alloy scattering is determined to be the dominant mechanism-limiting mobility; this enables us to extract an alloy-scattering parameter of $V_0=1.8$ eV for the $Al_xGa_{1-x}N$ material system. Polarization-doping presents an exciting technique for creating electron slabs with widely tunable density and confinement for the study of dimensionality effects on charge transport and collective phenomena.

DOI: 10.1103/PhysRevB.67.153306 PACS number(s): 73.61.Ey, 72.80.Ey, 81.10.Bk

A polar crystal with a spatially changing polarization $\mathbf{P}(\mathbf{r})$ will possess a fixed volume charge of density $\rho=\nabla\cdot\mathbf{P}(\mathbf{r})$. If sources of free carriers (electrons or holes) are available in the crystal, it is possible to use the field created by the bound polarization charge to *dope* the fixed volume charge region with neutralizing *mobile* charges. It is possible to experimentally realize such a system by alloying two materials of different polarizations and spatially varying the alloy composition (i.e., grading).

In a recent work,[1] we reported the realization of three-dimensional electron slabs (3DES) in graded $Al_xGa_{1-x}N$ semiconductor layers, using this technique of polarization doping. The III–V nitride family of crystals (GaN, AlN, InN) is well suited for polarization doping owing to the large spontaneous and piezoelectric polarizations.[2] The 3DES generated by this technique was found to possess the following characteristics: (a) the carrier density remains independent of temperature (no freezeout), (b) the mobility is *much higher* than the corresponding uniformly donor-doped carriers, especially at *low temperatures* (owing to the drastic reduction of ionized impurity scattering), and (c) the free carriers are *indeed* three dimensional from capacitance-voltage profiling. These properties make it a convenient system to study magnetotransport properties of the three-dimensional carrier systems. We have observed clearly resolved Shubnikov–de-Haas oscillations for such a polarization-doped 3DES. We are able to measure the (a) effective mass, (b) quantum scattering time, and (c) alloy-scattering potential for the 3DES electrons in $Al_xGa_{1-x}N$.

Figure 1 shows a schematic of charge control and band diagram of the technique of polarization doping that we have developed. Also shown in the figure is the sample structure we have used. The sample is a Ga-face structure grown by plasma-induced molecular-beam epitaxy[3] on a metal-organic chemical vapor deposition grown semi-insulating[4] GaN on a sapphire substrate. The growth is along the polar $c(0001)$ axis.[5] The top 100 nm of the structure is linearly graded $Al_xGa_{1-x}N$; the composition of Al is changed from 0% to 30% by controlling the aluminum flux by a computer program.[1] Grading over a layer thickness d creates the polarization dipole with fixed bulk charge $N_\pi^D=\nabla\cdot\mathbf{P}=\partial P(z)/\partial z$ and a fixed surface sheet charge $\sigma_\pi^S=\mathbf{P}\cdot\hat{\mathbf{n}}=|\mathbf{P}|$. The neutralizing dipole formed results in the 3DES; the schematic band diagram depicts this situation. The 3DES formed has a temperature-independent electron *sheet* density $n_{2d}=7.5\times10^{12}$ cm^{-2} and a mobility $\mu=2700$ cm^2/V s at $T=20$ K, measured by conventional low-B field Hall measurement.

For magnetotransport measurements of the 3DES, ohmic contacts were formed in a Vander Pauw geometry (Fig. 2

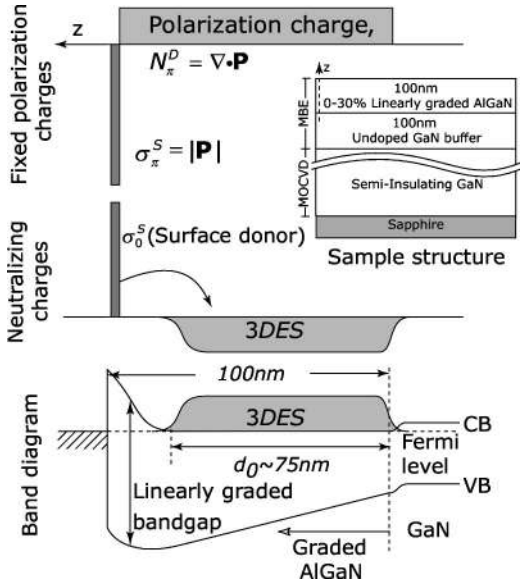

FIG. 1. Schematic of charge control showing polarization charges and formation of the 3DES. The band diagram shows depletion of the 3DES from the surface potential. Also shown is the epitaxial layer structure that is used to generate the 3DES.

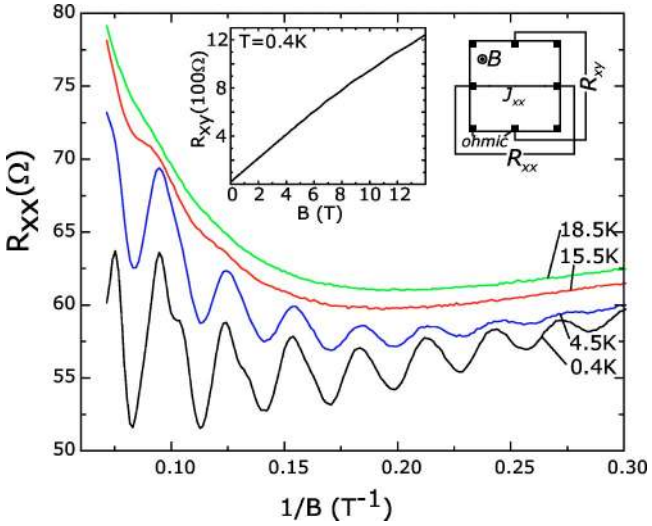

FIG. 2. Measured transverse magnetoresistance R_{xx} vs $1/B$ for different temperatures; the insets show measured R_{xy} vs B and the geometry used for the measurements.

inset). The sample was immersed in a ^{3}He low-temperature cryostat with a base temperature of 300 mK. Magnetic fields in the range $0\ \mathrm{T} \leqslant B \leqslant 14\ \mathrm{T}$ were applied. R_{xx} and R_{xy} was measured as in the geometry depicted in the figure using the standard low-frequency lock-in technique.

In Fig. 2, we plot the measured R_{xx} against $1/B$ for four temperatures. Also inset is the geometry of contacts and a plot of measured R_{xy} against B for $T=0.4$ K. The Hall mobility determined from the slope of the R_{xy} curve is $\mu_H \simeq 3000\ \mathrm{cm^2/V\,s}$. If the 3DES is spread over a thickness d_0, the sheet carrier density of the 3DES is calculated to be $n_{2d}=n_{3d}\times d_0=1/R_H e=B/eR_{xy}=7.2\times10^{12}\ \mathrm{cm^2}$. This is consistent with the low-field Hall-sheet density of $n_{2d}=7.5\times10^{12}\ \mathrm{cm^2}$. The spread of the 3DES is calculated from a self-consistent Poisson-Schrödinger band calculation to be $d_0=75$ nm, due to a 25 nm depletion of the 3DES from the surface potential (Fig. 1). This depletion in the graded $Al_xGa_{1-x}N$ layer has also been verified by capacitance-voltage profiling.[1] Thus, the Hall three-dimensional carrier density is $n_{3d}\sim10^{18}\ \mathrm{cm^3}$. The oscillations are periodic in $1/B$, and can be used to extract several parameters.

The oscillatory component of the transverse magnetoresistance component ΔR_{xx} is given by[6]

$$\Delta R_{xx}^{osc}=\frac{\chi}{\sinh\chi}e^{-\pi/\omega_c\tau_q}\left(\frac{\hbar\omega_c}{2\varepsilon_F}\right)^{1/2}\cos\left(\frac{2\pi\varepsilon_F}{\hbar\omega_C}\right), \qquad (1)$$

where $\chi=2\pi^2k_BT/\hbar\omega_c$, $\omega_c=eB/m^*$ is the cyclotron frequency, τ_q is the quantum scattering time, and $\varepsilon_F=\hbar^2k_F^2/2m^*$ is the Fermi energy with $k_F=(3\pi^2n_{3d})^{1/3}$.

The R_{xx} oscillation period $\Delta(1/B)=2e/\hbar(3\pi^2n_{3d})^{-2/3}=0.0294\ \mathrm{T^{-1}}$ gives a *direct* measurement[7] of the three-dimensional carrier concentration $n_{3d}=1.1\times10^{18}\ \mathrm{cm^{-3}}$, which is close to the carrier density inferred from the classical Hall and C-V measurements. Also, there is no observable change in the oscillation period with changing magnetic field, indicating the absence of magnetic freezeout[8] effects.

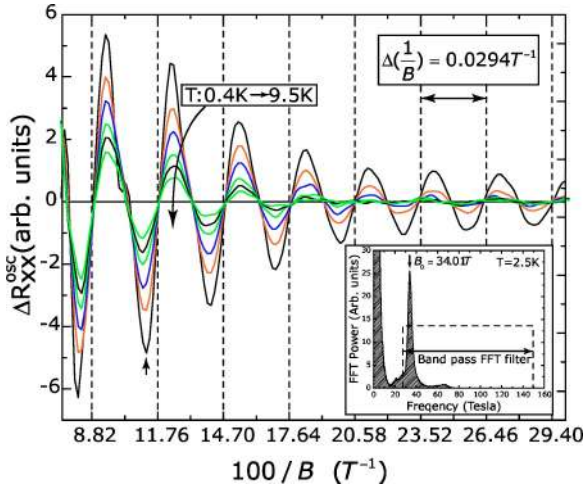

FIG. 3. The oscillatory component ΔR_{xx}^{osc} plotted against $1/B$. The oscillations are periodic with a period $\Delta(1/B)=0.0294\ \mathrm{T^{-1}}$, and are damped with both increasing temperature (different curves) and increasing $1/B$. Also shown in the inset is a typical FFT power spectrum (at $T=2.5$ K) showing a peak at the fundamental period, and the band-pass window used to filter the oscillatory component ΔR_{xx}^{osc}.

For analysis of the oscillatory part ΔR_{xx}, the background is removed using standard Fast Fourier Transform (FFT) techniques; the resulting ΔR_{xx} for various temperatures $0.4\ \mathrm{K}<T<9.5\ \mathrm{K}$ is plotted against $1/B$ in Fig. 3. A typical FFT power spectrum (at $T=2.5$ K) is shown in the inset. There is a clearly resolved peak at the fundamental oscillation period $B_0=34.01$ T, and a weak second harmonic.[9]

The effective mass of carriers is determined by fitting[10] the measured amplitude damping [Fig. 4(a)] with temperature at fixed B to the temperature-damping term of Eq. (1), $\chi/\sinh\chi$. For the peak at $B=8.9$ T (arrow in Fig. 3), the effective mass is found to be $m^*=0.21m_0$; we get the same effective mass for the amplitude peaks at $B=10.5$ T. The band-edge electron effective mass in pure GaN (AlN) is $m^*_{GaN}=0.20m_0(m^*_{AlN}=0.32m_0)$.[11] From a linear interpolation for the 3DES experiencing an average Al composition of $\langle x\rangle=0.11$, we expect an effective mass of $0.21m_0$, which is in good agreement with the measured value. The value is

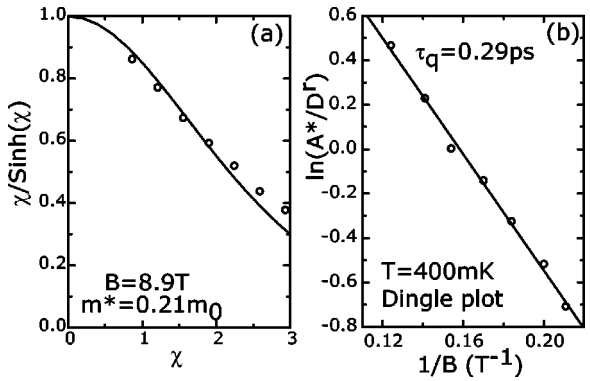

FIG. 4. (a) Effective-mass plot at $B=8.9$ T, where the data (dots) are fit to the $\chi/\sinh\chi$ (line) damping term (Ref. 10). (b) Dingle plot for extraction of the quantum scattering time (Ref. 13).

TABLE I. Summary of constants used and results extracted from magnetoresistance measurements

Quantity	Symbol	Magnitude	Unit
Relative dielectric constant	ϵ_r	8.9 (GaN), 8.5 (AlN)	
Lattice constant	a_0	3.189 (GaN), 3.112 (AlN)	Å
Lattice constant	c_0	5.185 (GaN), 4.982 (AlN)	Å
Effective mass	m^*	0.21	m_0
Quantum scattering time	τ_q	0.3	ps
Transport scattering time	τ_m	0.34	ps
3DES density	n_{3d}	1.1×10^{18}	cm^{-3}
3DES Hall mobility (1K)	μ_H	3000	$cm^2/V\cdot s$
Alloy scattering potential	V_0	1.8	eV

close to the effective mass measured for two-dimensional electron gases at $Al_xGa_{1-x}N/GaN$ heterojunctions by the Shubnikov de–Haas method.[12]

From Eq. (1), the slope of the Dingle plot[13] [Fig. 4(b)], i.e., $\ln[A^*/(\sqrt{\hbar\omega_c/2\varepsilon_F}\chi/\sinh\chi)]$ (A^* stands for peak values of the oscillation) plotted against $1/B$ yields a quantum scattering time of $\tau_q=0.29$ ps. An averaging of the quantum scattering times over a range of low temperatures yields a value $\tau_q^{av}=0.3$ ps.

Distinct from the quantum scattering time is the "classical" (or momentum) scattering time τ_c which is directly measured from mobility via the Drude relation $\mu=e\tau_c/m^*$. Low-temperature Hall mobility gives $\tau_c=0.34$ ps for the 3DES. Within limits of experimental error, the ratio $\tau_c/\tau_q\sim1$. For *isotropic* scattering, it is well known[14] that $\tau_c/\tau_q\approx1$. On the other hand, $\tau_c/\tau_q\gg1$ for scattering that peaks at small angles—scattering from Coulombic impurities is of this form. Thus, the ratio indicates that the dominant scattering mechanism at low temperatures is probably[15] of a short-range (isotropic) nature.

Size-effect scattering[16] that occurs if the width of the 3DES is much less than the mean-free path of electrons is negligible since our 3DES has a mean-free path $\lambda=\hbar k_F\mu/e\approx60$ nm, whereas the width of the 3DES is $d_0\approx75$ nm. The chief scattering mechanisms that can affect mobility are alloy disorder scattering, charged dislocation scattering (owing to a high density of dislocations $N_{disl}\sim10^9$ cm^{-2}), and ionized impurity scattering from the remote donors at the surface states.

Hsu and Walukiewicz[15] show that remote ionized impurity scattering strongly favors small-angle scattering, thus causing the ratio $\tau_c/\tau_q\gg1$. Since $\tau_c/\tau_q\approx1$ for our 3DES, remote ionized impurity scattering is unimportant.

The ratio of classical to quantum scattering times due to charged dislocation scattering was recently calculated[17] to be

$$\frac{\tau_c}{\tau_q}\Big|_{disl}=1+2k_F^2\lambda_{TF}^2, \tag{2}$$

where $\lambda_{TF}^2=2\epsilon\varepsilon_F/3e^2n_{3d}$ is the Thomas-Fermi screening length of the degenerate 3DES. The ratio for our 3DES is 2.3; thus, we exclude dislocation scattering to be the most important scattering mechanism.

So we converge on alloy scattering as the dominant scattering mechanism at low temperatures. Alloy-scattering potential V_0 is of a short-range nature, which makes the scattering process isotropic and $\tau_c/\tau_q\sim1$, as observed. The scattering rate due to alloy disorder with a short-range potential V_0 for a degenerate 3DES is given by[7]

$$\frac{1}{\tau_{alloy}}=\frac{2\pi}{\hbar}V_0^2\Omega(x)x(1-x)g_{3D}(\varepsilon_F), \tag{3}$$

where $\Omega_0(x)$ is alloy composition-dependent volume of the unit cell over which the alloy-scattering potential V_0 is effective, and x is the alloy composition. $g_{3D}(\varepsilon)$ is the three-dimensional density of states. Besides, the alloy is graded, and Matheissen's rule, which is accurate for low-temperature transport analysis is used for a spatial averaging of the scattering rate

$$\langle\tau_{alloy}^{-1}\rangle=\frac{1}{x_0}\int_0^{x_0}\tau_{alloy}^{-1}(x)dx, \tag{4}$$

where $x_0=0.225$ is the alloy composition experienced by the 3DES electrons at the top edge of the depletion region. Using this simple result and the material constants of GaN and AlN in Table I, we conclude that to achieve a low-temperature transport mobility of 3000 cm^2/V s, an alloy-scattering potential of $V_0=1.8$ eV is necessary. Due to the lack of experimental values, it is common practice to assume the scattering potential to be the conduction band offset between the binaries forming the alloy ($V_0=\Delta E_c=2.1$ eV for AlN, GaN).[11] With an alloy scattering potential of $V_0=2.1$ eV, the calculated mobility is *much lower* (≈2000 cm^2/V s) than the measured value. Besides, our 3DES mobility is dominated by alloy scattering and all other scattering mechanisms are removed, making it a clean measurement of the alloy-scattering potential. This report presents the *first measurement* of the alloy-scattering potential in $Al_xGa_{1-x}N$ material system.

In summary, we demonstrated Shubnikov–de-Haas oscillations of a degenerate three-dimensional electron gas realized by the technique of polarization bulk doping. It resulted in the measurement of the effective mass of electrons in the graded $Al_xGa_{1-x}N$ layer ($m^*=0.21m_0$) and their quantum scattering time ($\tau_q=0.3$ ps). Alloy scattering was identified as the dominant scattering mechanism from the measured

ratio of classical and quantum scattering times, making it possible to measure the alloy-scattering potential ($V_0 = 1.8$ eV).

Finally, we mention that degenerate three-dimensional electron gases are an interesting playground for the study of collective phenomena such as spin-density waves, Wigner crystallization, and integral and fractional quantum-Hall effects in three dimensions.[18] Polarization-doped electron slabs presented in this work provide an interesting addition to the few existing techniques[19] of creating such electron populations, overcoming the thermal freezeout effects associated with *impurity-doped* semiconductors. The wide *tunability* of slab thickness and electron density offered by polarization-doping makes it an attractive system to study such effects.

The authors would like to thank Jasprit Singh and Herbert Kroemer for useful discussions, and Huili Xing for a critical reading of the manuscript. Funding from POLARIS/MURI (Contract monitor: C. Wood) is gratefully acknowledged.

*Electronic address: djena@engineering.ucsb.edu

[1] D. Jena *et al.*, Appl. Phys. Lett. **81**, 4395 (2002).
[2] F. Bernardini, V. Fiorentini, and D. Vanderbilt, Phys. Rev. B **56**, R10 024 (1997).
[3] B. Heying, R. Averbeck, L.F. Chen, E. Haus, H. Riechert, and J.S. Speck, J. Appl. Phys. **88**, 1855 (2000).
[4] S. Heikman, S. Keller, S.P. DenBaars, and U.K. Mishra, Appl. Phys. Lett. **81**, 439 (2002).
[5] P. Waltereit *et al.*, Nature (London) **406**, 865 (2000).
[6] R. Kubo, H. Hasegawa, and N. Hashitsume, J. Phys. Soc. Jpn. **14**, 56 (1959).
[7] C. Hamaguchi, *Basic Semiconductor Physics* (Springer-Verlag, Berlin, 2001).
[8] K. Seeger, *Semiconductor Physics, An Introduction* (Springer-Verlag, Berlin, 1999), P. 307.
[9] Harmonics appear since the measured oscillations are not perfect sinusoids. Neglecting the weak second harmonic introduces no appreciable error. We use a $N=2^{15}$ size FFT window and a $f_{pass}=28-150$ T band-pass filter to remove the background component.
[10] R.J. Sladek, Phys. Rev. **110**, 817 (1958).
[11] I. Vurgaftman, J.R. Meyer, and L.R. Ram-Mohan, J. Appl. Phys. **89**, 5815 (2001).
[12] S. Elhamri *et al.*, Phys. Rev. B **57**, 1374 (1998).
[13] R.B. Dingle, Proc. R. Soc. London, Ser. A **211**, 517 (1952).
[14] J.P. Harrang, R.J. Higgins, R.K. Goodall, P.R. Ray, M. Laviron, and P. Delescluse, Phys. Rev. B **32**, 8126 (1985).
[15] L. Hsu and W. Walukiewicz, Appl. Phys. Lett. **80**, 2508 (2002).
[16] W. Walukiewicz, P.F. Hopkins, M. Sundaram, and A.C. Gossard, Phys. Rev. B **44**, 10 909 (1991).
[17] D. Jena and U.K. Mishra, Phys. Rev. B **66**, 241307(R) (2002).
[18] B.I. Halperin, Jpn. J. Appl. Phys. **26**, Suppl. 3 (1987).
[19] A.C. Gossard, M. Sundaram, and P.F. Hopkins in *Epitaxial Microstructures*, edited by A.C. Gossard, Semiconductors and Semimetals Vol. 40 (Academic, San Diego, 1994).